Adaptive Control for Hybrid Underwater Gliders

Ottmar Rafael Uriza Gosebruch.
Automatic Control Department, CINVESTAV. México D.F., México.
ottmar.uriza@cidesi.edu.mx

Tomas Salgado-Jimenez
Research Department, CIDESI, Querétaro., México.
tsalgado@cidesi.edu.mx

Jorge Torres Muñoz.
Automatic Control Department, CINVESTAV. México D.F., México.
jtorres@ctrl.cinvestav.mx

Eduardo Campos Mercado.
Automatic Control Department, CINVESTAV. México D.F., México.
ecampos@ctrl.cinvestav.mx

Luis G. Garcia-Valdovinos
Research Department, CIDESI, Querétaro., México.
ggarcia@cidesi.edu.mx

***Abstract* – This paper was developed by the Department of Automatic Control, CINVESTAV in collaboration with the Center for engineering and Industrial Development CIDESI, Querétaro. This document involves the design and construction of a hybrid underwater Glider. The control objective is to follow a trajectory that is currently implemented by commercial gliders. The dynamic model is used to propose a control strategy based on functions of energy. The used control strategy used is an adaptive control, known as the algorithm of Slotine-Li in its Adaptive version and for the stability proof a candidate Lyapunov function was used. Finally it should be mentioned that we have results on simulation and real-time experiments. In addition the Gliders model is expressed in a matrix form.**

Keywords: Underwater Glider, Adaptive control, Hybrid underwater Glider.

I. INTRODUCTION

Underwater gliders are underwater vehicles that not use an external active propulsion system. Commercially available gliders such as the Slocum (Webb, 2001;),and the Seaglider (Eriksen, 2001;), are capable of long range missions with low energy consumption, low cost and great endurance. These characteristics are also applicable for the Spray (Sherman, 2001;), although is not commercially available for the moment. They have found broad application in physical and biological oceanography. With careful design, buoyancy driven gliders are quiet and use a minimum power (Leonard and Graver, 2001; Rogers, 2004; Graver, 2005; Kanetal, 2008; Arima, 2008; Seo, 2008).

Underwater gliders can be used in remote sensing applications for physical, chemical and biological oceanography. The implemented vehicle has an actuation system combining those of autonomous gliders and the propulsion AUVs. Since Alvarez et al (2004), the research work has increased in this type of AUV and have proposed development of small-size, inexpensive Gliders with design focused on specific goals.

In order to understand the underwater glider system dynamics and its related properties, an accurate mathematical model that represents the system is highly needed. Accordingly, it is desirable to determine the equations of motion of the prescribed vehicles and take advantage of the vehicle's geometrical properties. In this paper we take as a cylindrically actuated moving mass, which matches the mechanization of several existing gliders including Seaglider (Eriksen , 2001), Spray (Sherman, 2001), and a glider recently developed at Virginia Tech (Wolek , 2012). The Glider mathematical modelling was based in the work designed by Leonard and Graver (2001) and Graver (2005).

The equation of motion for underwater gliders is derived from the first principle to consider the major design elements including buoyancy control, and internal mass actuators. However, this model has a disadvantage that is not as simple to propose a control algorithm as in other models. In order to simplify the proposal of a control, the mathematical equations of motion of the system, is expressed in a well-known equation for underwater vehicle systems; the Fossen's generic equation (Fossen, 1994-2002).

The control technique used in this article is an adaptive control law, which is the Slotine – Li algorithm in its adaptive version, which the main goal to adapt those parameters that are difficult to determine or with a lot of uncertainty, in addition the adaptive law reduce the possibility of an erroneous modelling of the underwater glider system, although the information obtained from the control law will provide a more transparent overview of glider system dynamics and properties.

The adaptive law uses an energy function to adapt the parameters and also the Lyapunov candidate function provides the stability of the mechanical systems. Energy-based design methodologies, such as the method of controlled Lagrangians (Bloch, Leonard, & Marsden, 2000) and the method of interconnection and damping assignment (Ortega, Spong, Gomez-Estern, & Blankenstein, 2002), provide systematic procedures for choosing control laws for mechanical systems such that the closed-loop dynamics. The energy of the closed-loop system serves as a control Lyapunov function. The gains of the control law and the adaptive law can be adjusted to make a bigger region of attraction for the closed-loop system.

II. MODELLING

The main elements of the mathematical model are: the vehicle configuration, its geometry, the gravity forces and buoyancy, the added mass effects, the inertia moment because of the movement and the fluid density, the hydrodynamic force, including the lift, drag and moment, and the nonlinear coupling between the internal mass and the ballast system. This model results from the analysis of moments and the Newton´s law (Leonard and Graver et al., 2001), in addition the three equations of the three degrees of freedom are expressed in a matrix equations (Fossen et al., 2002). This matrix structure makes easier to propose a control law.

2.1. Vehicle’s kinematic.

The kinematics of the vehicle can be explained based on Fig. 1 (Leonard and Graver et al., 2001). Consider an inertial frame *i, j* and *k*. Let *i* and *j* inertial axes lie in the horizontal axis perpendicular to gravity. The *k* axis lies in the direction of the gravity vector and is positive downwards and the value for *k=0* coincides with the water surface, and *k* is the depth.

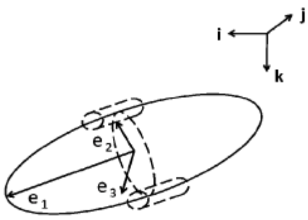

Figure 1.The inertial frame and the body frame.

The orientation of the vehicle is given by the rotation matrix **R**, which maps vectors expressed in the body frame in to internal body coordinates. Yaw, pitch and roll are the three rotation angles from the inertial body frame. The position of the vehicle, $= (x \quad y \quad z)^T$, expressed in the inertial frame. The vehicle moves with translational velocity $v = (v_1 \quad v_2 \quad v_3)^T$ and the angular velocity as $\Omega = (\Omega_1 \quad \Omega_2 \quad \Omega_3)^T$ as shown in Fig. 2.

$$\dot{R} = \Omega \times R$$
$$\dot{b} = Rv$$

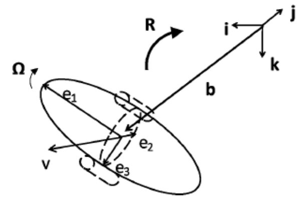

Figure 2. Glider position and orientation variables.

2.2. Leonard – Graver dynamic.

The vehicle has buoyancy control and controlled internal moving mass that will manipulate the CB to change the glide angle and speed. The total mass of the vehicle mass can be defined by the next equation; all the components are described in Fig. 3:

$$m_v = m_h + m_w + m_b + \bar{m}.$$

(m_v): Total mass.

(m_h , r_h): Hull mass and the vector referred to the center of buoyancy.

(m_w, r_w): Compensation mass and its vector referred to the center of buoyancy.

(m_b , r_b): Ballast mass and its vector referred to the center of buoyancy.

($\bar{m}$, r_p): Movable mass and its vector referred to the center of buoyancy.

So that the vehicle is negatively buoyant if the value of m_o is positive (downward motion) and it is positively buoyant if the value of m_o) is negative (upward motion).

$$m_o = m_v + m$$

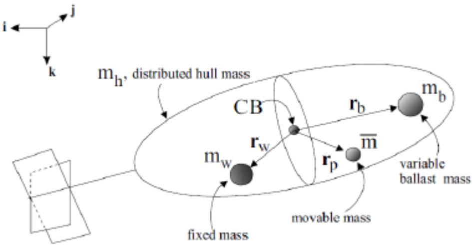

Figure 3. Masses and vectors of the vehicle.

2.3. Motion in the vertical plane

The main assumption in the vertical plane is to ignore certain associated dynamics. In the dynamic equation, the vertical plane can be classified as an invariant plane. In this paper, the vertical plane dynamics are controlled using movable mass and variable ballast mass. Thus, it is assumed that all the lateral components such as v_2 are small and close to zero except for the pitching component Ω_2. It is also assumed that the higher order terms of the damping matrix can be neglected. In order to simplify the equation of motion of the underwater vehicle the off-diagonal terms and coupling terms are neglected, as well as assuming a constant added mass (Smallwood andWhitcomb,2001; Fossen, 2002). Also with the assumption that the external geometry of the glider planes is symmetry, the contribution of wing is dominated by the lift and drag forces during low angle of attack. The ballast mass is fixed at the center of mass of the vehicle which coincide in two axes with the center of the movable mass. Accordingly r_p and r_b values have only one component and it is possible to eliminate the inertial coupling effect due to the offset static point mass, mw and the coupling between the ballast state and the vehicle inertia pitch moment.

The model to the vertical plane can be simplified as:

$$R = \begin{bmatrix} C & 0 & -S \\ 0 & 1 & 0 \\ S & 0 & C \end{bmatrix}$$

$$b = \begin{pmatrix} x \\ 0 \\ z \end{pmatrix}; v = \begin{pmatrix} v_1 \\ 0 \\ v_3 \end{pmatrix}; \Omega = \begin{pmatrix} 0 \\ \Omega_2 \\ 0 \end{pmatrix};$$

$$r_p = \begin{pmatrix} r_{p1} \\ 0 \\ 0 \end{pmatrix}; r_b = \begin{pmatrix} r_{b1} \\ 0 \\ 0 \end{pmatrix};$$

$$P_p = \begin{pmatrix} P_{p1} \\ 0 \\ 0 \end{pmatrix}; P_b = \begin{pmatrix} P_{b1} \\ 0 \\ 0 \end{pmatrix}; P_w = u_w = \begin{pmatrix} 0 \\ 0 \\ 0 \end{pmatrix};$$

$$F_{hydro} = \begin{pmatrix} -D \\ 0 \\ -L \end{pmatrix}; M_{hydro} = \begin{pmatrix} 0 \\ M_{DL2} \\ 0 \end{pmatrix};$$

$$\bar{u} = \begin{pmatrix} \bar{u}_1 \\ 0 \\ 0 \end{pmatrix}; u_b = \begin{pmatrix} u_{b1} \\ 0 \\ 0 \end{pmatrix};$$

The final equations in the vertical plane are as follows:

$$\dot{v_1} = \frac{1}{m_1}(-m_3 v_3 \Omega_2 - m_0 g \sin - D \cos\alpha\,({v_1}^2 + {v_3}^2) + L \sin\alpha\,({v_1}^2 + {v_3}^2) - u_1 - u_{b1}) \qquad (1)$$

$$\dot{v_3} = \frac{1}{m_3}(\bar{m}\, \dot{r_{P1}} \Omega_2 + (\bar{m} + m_b + m_1) v_1 \Omega_2 + m_0 g \cos - (L \cos\alpha + D \sin\alpha)({v_1}^2 + {v_3}^2) \qquad (2)$$

$$\dot{\Omega_2} = \frac{1}{J_2}((m_3 - m_1 - \bar{m} - m_b) v_1 v_3 - v_3 \bar{m}\, \dot{r_{P1}} + (\bar{m} g r_{P1} - m_b r_{b1}) \cos + M_{DL}({v_1}^2 + {v_3}^2 + {\Omega_2}^2) \qquad (3)$$

2.4. Fossen's dynamic.

The three equations above could be expressed as a matrix view, the next equations shows that:

$$M\dot{v} + C(v) + D(v) + g(\eta) = g_0 + g_m + w + f_m \qquad (4)$$

Where:

M – Inertia Matrix
C – Coriolis Matrix
D – Hydrodynamic Damping
g – Restoring and buoyancy forces
g_0, g_m Control for ballast systems and movable systems.
f_m - Propulsion of the actuators

$$M\dot{v} = \begin{bmatrix} m_1 & 0 & 0 \\ 0 & m_3 & 0 \\ 0 & 0 & J_2 \end{bmatrix} \begin{bmatrix} \dot{v_1} \\ \dot{v_3} \\ \dot{\Omega_2} \end{bmatrix}$$

$$C(v)v = \begin{bmatrix} 0 & 0 & m_3 v_3 \\ 0 & 0 & -v_1 m_t - \bar{m}\, \dot{r_{p1}} \\ -m_3 v_3 & v_1 m_t + \bar{m} \dot{r_{p1}} & 0 \end{bmatrix} \begin{bmatrix} v_1 \\ v_3 \\ \Omega_2 \end{bmatrix}$$

Where:

$$m_t = m_1 + m_b + \bar{m}$$

$$D(v)v = \begin{bmatrix} (D\ C\alpha)(v_1) & 0 & 0 \\ 0 & (D\ S\alpha)(v_3) & 0 \\ 0 & 0 & M_{DL}\Omega_2 \end{bmatrix} \begin{bmatrix} v_1 \\ v_3 \\ \Omega_2 \end{bmatrix}$$

$$g(\eta) = \begin{bmatrix} m_0 g\ S \\ -m_0 g\ C \\ \bar{m} g r_{P1} C - (m_b r_{b1} C) \end{bmatrix}$$

$$g_m = \begin{bmatrix} -u_1 \\ 0 \\ 0 \end{bmatrix}; \quad g_0 = \begin{bmatrix} -u_{b1} \\ 0 \\ 0 \end{bmatrix}; \quad f_m = \begin{bmatrix} f_m \\ 0 \\ 0 \end{bmatrix};$$

Transforming in to the inertia frame, by the next equation:

$$\dot{\eta} = J(\eta) v \ \Rightarrow\ v = J(\eta)^{-1} \dot{\eta} \qquad (5)$$

Where:

$$J(\eta) = \begin{bmatrix} C & S & 0 \\ -S & C & 0 \\ 0 & 0 & 1 \end{bmatrix}$$

And replacing (5) into (4), we obtain the final equation that represent the open loop system, which is shown as follows:

$$M_\eta(\eta)\ddot{\eta} + C_\eta(v,\eta)\dot{\eta} + D_\eta(v,\eta)\dot{\eta} + g^{\circ}(\eta) = f_{m\eta}(\eta) \qquad (6)$$

Where:

$$M_\eta(\eta) = J^{-1}(\eta) M J^{-T}(\eta)$$

$$C_\eta(v,\eta) = J^{-1}(\eta)\left[C(v) - J^{-1}(\eta)\dot{J}(\eta) M\right] J^{-T}(\eta)$$

$$D_\eta(v,\eta) = J^{-1}(\eta) D(v,\eta) J^{-T}(\eta)$$

$$f_{m\eta}(\eta) = J^{-1}(\eta)(g_0 + g_m + w + f_m)$$

$$g^{\circ}(\eta) = J^{-1}(\eta) g(\eta)$$

III. CONTROL LAW

The system equation in closed loop is:

$$M_\eta(\eta)\ddot{\eta} + C_\eta(v,\eta)\dot{\eta} + D_\eta(v,\eta)\dot{\eta} + g^\circ(\eta) = \tau_\eta + f_{m\eta}(\eta) \quad (7)$$

For notation simplicity the arguments of the matrices and vectors in the last equation will be expressed as follows:

$$M_\eta(\eta) = M_\eta$$

$$C_\eta(v,\eta) = C_\eta$$

$$D_\eta(v,\eta) = D_\eta$$

$$g^\circ(\eta) = g^\circ$$

$$f_{m\eta}(\eta) = f_{m\eta}$$

In the adaptive algorithm of Slotine- Li we need the use of some virtual variables, V_A & r being the last one a function of the system error, the variables and its derivatives are shown below:

$$V_A = \dot{\eta}_d - \Delta(\eta - \eta_d) \quad (8)$$

$$r = \dot{\eta} - V_A \quad (9)$$

$$r = \dot{\eta} - \dot{\eta}_d + \Delta(\eta - \eta_d) = \dot{e} + \Delta(e)$$

The control algorithm is established as follows:

$$\tau_\eta = Y(v,\eta,V_A,\dot{V}_A)\hat{p} - KD * r - f_{m\eta}(\eta) \quad (10)$$

Substituting the control input (10) into (7) and defining the parametric error as the estimate parameter minus the real parameter value, this is shown in equation (11) and gathering the terms with a change of variable in function of the error r we finally obtain the matrix regressor of the approximately parameters showed in equation (12):

$$\tilde{p} = \hat{p} - p$$

$$M_\eta\dot{r} + C_\eta r + D_\eta r + KDr = Y(v,\eta,V_A,\dot{V}_A)\tilde{p} \quad (11)$$

Where:

$$Y(v,\eta,V_A,\dot{V}_A)\tilde{p} = \widetilde{M_\eta}\,\dot{V}_A + \widetilde{C_\eta}V_A + \widetilde{D_\eta}V_A + \widetilde{g^\circ}$$

For simplicity:

$$Y(v,\eta,V_A,\dot{V}_A)\tilde{p} = Y\tilde{p}$$

IV. STABILITY PROOF

To define the stability of the system in closed loop, we propose the next Lyapunov function candidate:

$$V = \tfrac{1}{2}r^T M_\eta r + \tfrac{1}{2}\tilde{p}^T\gamma\tilde{p} \quad (12)$$

Then along solution trajectories it follows that.

$$\dot{V} = -\,r^T\left[D_\eta + KD\right]r + \tilde{p}^T[Y^T r + \gamma\,\dot{\tilde{p}}] \quad (13)$$

If we choose the parameter adaptation law in equation (13) to make the second term zero:

$$\dot{\tilde{p}} = \dot{\hat{p}} = -\gamma^{-1}\,Y^T r$$

Then

$$\dot{V} = -\,r^T\left[D_\eta + KD\right]r \le 0 \quad (14)$$

Remember that $D_\eta = {D_\eta}^T > 0$ and $K_D = {K_D}^T > 0$, then this function is shown that is bounded and it will always decrease by any r value increment. Therefore the stability of the equilibrium point is guaranteed. In order to prove the asymptotic stability in (15), the Krasovskii-LaSalle's theorem can be used. The Krasovskii – LaSalle's lemma states that given a representation of the system $\dot{x} = f(x)$ where x is the vector of variables, with$f(0) = 0$, being a $V(x)$ can be found such that:

$V(x) > 0$ For all $x \neq 0$.(Positive definite)

$\dot{V}(x) \le 0$ For all x. (Semi negative semi definite)

$V(x) \to \infty$ If $x \to \infty$ & $V(0) = \dot{V}(0) = 0.$

Let τ be the union of complete trajectories contained entirely in the set$\{x : \dot{V}(x) = 0\}$. Then the set of accumulation points of any trajectory is contained in τ. In particular, if τ contains no trajectory of the system except the trivial trajectory $x(t) = 0$ for$t \ge 0$, then the origin is globally asymptotically stable.

So:

$$\dot{V} = 0$$

And this is possible if and only if:

$$r = \dot{e} + \Delta(e) = 0 \quad \Leftrightarrow \quad e = 0$$

Thereby we can conclude that the system is asymptotically stable.

V. SIMULATION

Before the real time experiments it is necessary to prove that the system in closed loop is stable and our control algorithm is stable, as well the adaptive control is working and the adaptive parameters that were estimated converge to a constant value.

There are difference between the simulation and the real time experiments, the first one is that the Set points for Pitch angle and z are sinusoidal trajectories in the simulation, and fixed values in real time experiments. And the most important difference between simulation results and experiment results were the total of parameters that were adapted are 3 for each degree of freedom (Pitch, Z).

In addition it is necessary to mention that the state X is an uncontrolled degree of freedom. To obtain the results, we consider a constant velocity in the translational movement of X. The simulation results are shown in the next images.

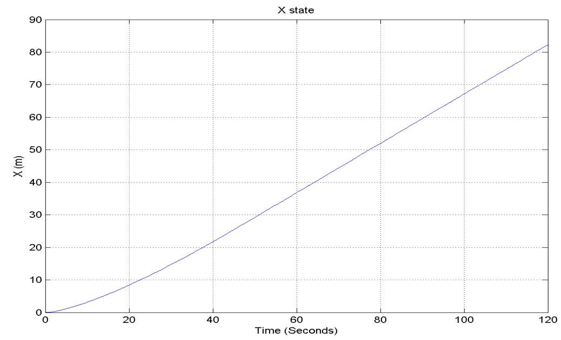

Figure 4. Translational movement in X.

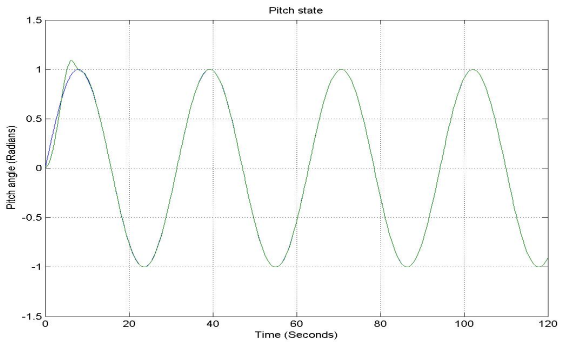

Figure 5. Response in Pitch.

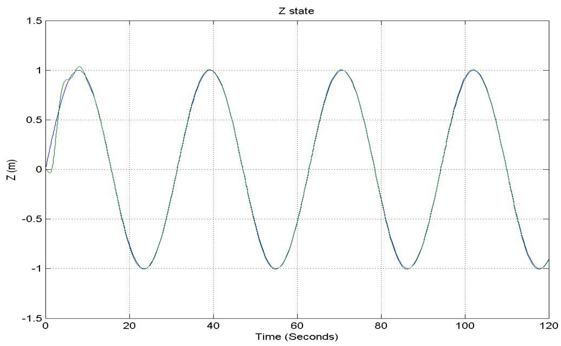

Figure 6. Response in z.

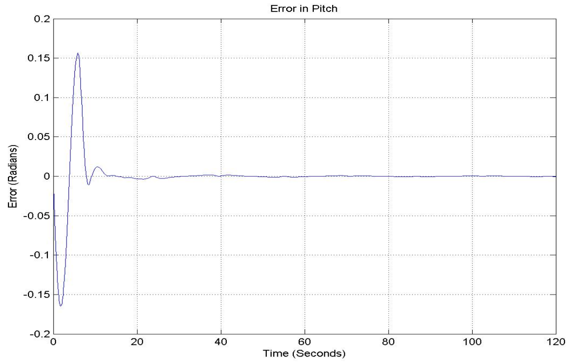

Figure 7. The error in Pitch.

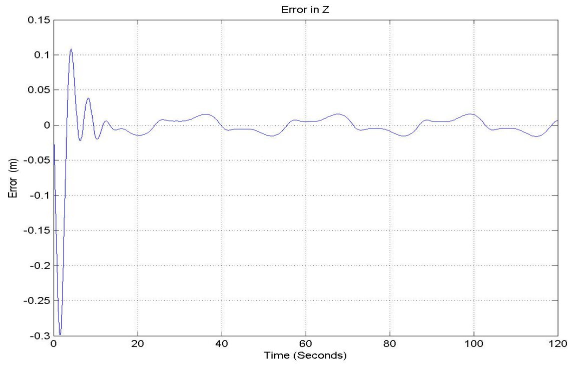

Figure 8. The error in z.

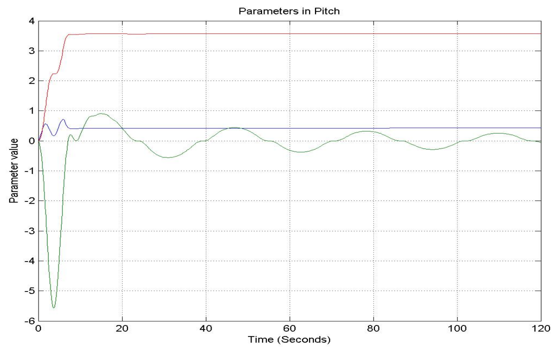

Figure 9. Parameters in Pitch.

	Estimated value
Parameter 1 (θ)	$\widehat{M_{DL}} = 0.53016$
Parameter 2 (θ)	$\widehat{m}_{t\theta} = 3.815$
Parameter 3 (θ)	$\widehat{J_2} = 0.1023$

Table 1. The parameters value of simulation (Pitch).

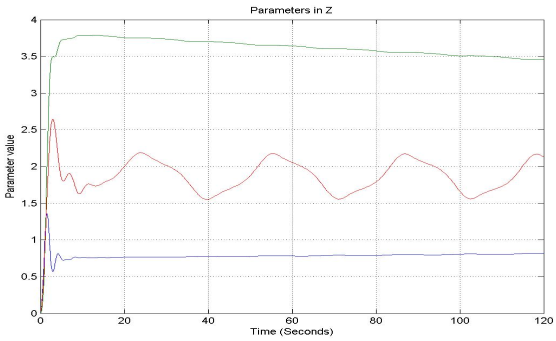

Figure 10. Parameters in Z.

	Estimated value
Parameter 1 (z)	$\widehat{W}_Z = 0.74107$
Parameter 2 (z)	$\widehat{m}_z = 2.294\ kg$
Parameter 3 (z)	$\widehat{H}_Z = 3.5124$

Table 2. The parameters value of simulation (z).

As could be appreciated in the simulations results, the control law stabilizes the system in closed loop proving that the adaptive law is working and ready to be prove in a real environment, with the specific constrains.

Most of all the parameters converge to a perfect constant value when the system passed to stationary time, showing that the adaptive algorithm works as we were waiting. In addition the systems converge to the Set point since the beginning, this is because the PD control acts in the firsts instances ensuring that the system could follow the trajectory and then when the adaptive control had been adjust and the parameters of the system are known, all the control were support by the adaptive algorithm. And finally in the error graphs are showed that the error decreased asymptotically, guarantying the asymptotically stability of the system using that control law.

VI. EXPERIMENTAL PROTOTYPE

This chapter describes how the prototype was constructed, the first part is the geometry of the vehicle and it mechanics systems. The geometry of the vehicle had been chosen quite similar to the commercial gliders as Slocum and Spray. The next image shows that.

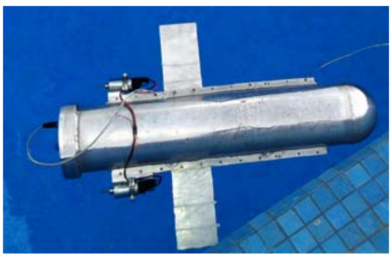

Figure 11. The prototype that has been developed.

The Ballast system and the movable mass have special actuators and special PWM outputs for each one. Their main characteristics are described of the actuators of each systems were fed with 5 volts and each have feedbacks, the ballast system has a Hall sensor that will provides the mass of the tank (m_b) and the linear actuator for the movable mass provides the positon (r_{P1}) of the mass ($\overline{m}$) .

The sensors that were used to read the Euler angle (Pitch) and the depth (z) were the IMU CH-LT6 and BMP085 respectively. The Inertial measurement unit UM6 – LT develops with serial communication, with 3.3 TTL volts and a speed rate up to 115200 Bauds. And the depth sensor develops with I2C communication, with 5 TTL volts and with an adjustable analogic clock. Although the control loop and the data acquisition were programed in an Arduino microcontroller, that is an embedded system with a C environment. Each Arduino has several ports for communication and PWM outputs. The internal structure of the Glider is shown below, also in the block diagram is including how the control law works:

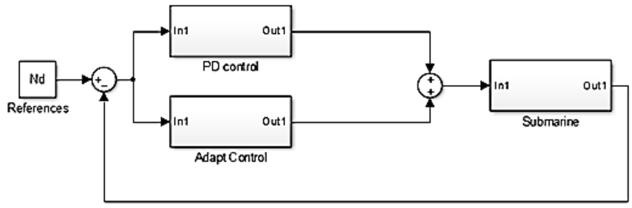

Figure 12. The closed loop system.

VII. EXPERIMENTAL RESULTS

The experimental results were obtained in the Polytechnique National Institute from Mexico City. The experiments were to probe the functionality of the movable mass ($\overline{m}$) and the adaptive control in only one degree of freedom (Pitch) with the adaptation of two parameters, and to reach several points using the immersion control with the only work of the ballast (m_b), and with the adaptation of only one parameter. This move is defined downward as negative, upward as positive.

The Glider´s set points were a series of diverse inputs, or changing set points in both of the degrees of freedom and were controlled in a simultaneously way. The main goal was to show the glide of the underwater glider. Because of the absence of currents in the pool system was acted in order to have propulsion and an X move. The results also include the graphs of the stationary error, the control evolution in time and the value of the estimated parameters.

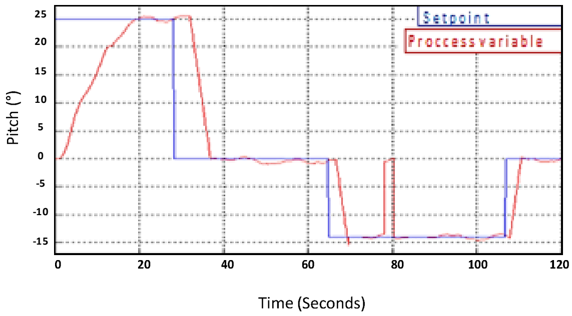

Figure 13. Pitch response in real time experiments.

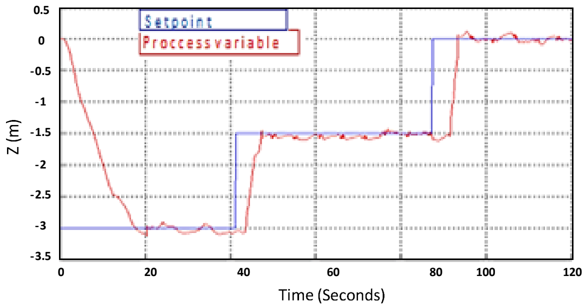

Figure 14. Z response in real time experiments.

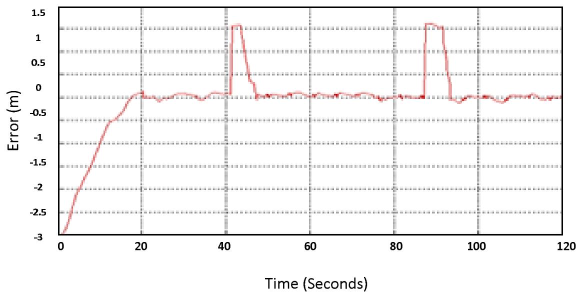

Figure 15. Depth error in real time experiments.

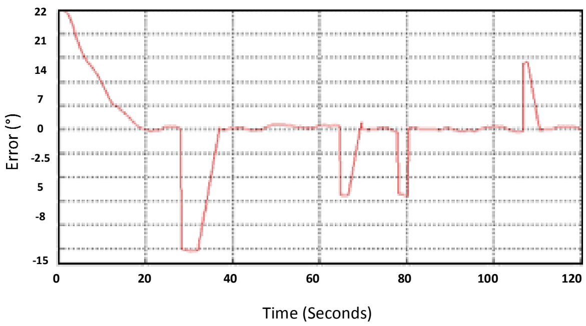

Figure 16. Pitch error in real time experiments.

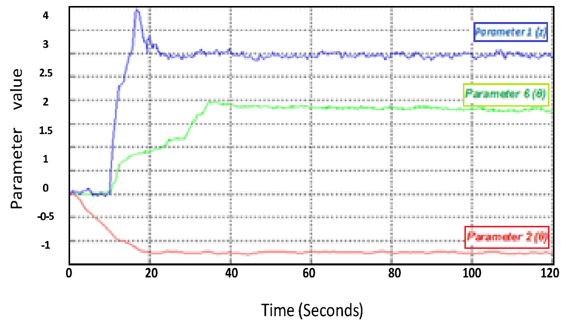

Figure 17. The estimation of the parameters.

	Estimated value
Parameter 1 (z)	$\widehat{m}_t * g = 3.051\ kg$
Parameter 2 (θ)	$\widehat{J}_2 = -1.2526$
Parameter 6 (θ)	$\widehat{m}_0 = 1.7108\ kg$

Table 3. Parameters value for the real time experiments.

VIII. Conclusions.

The experimental results shows that the adaptive Slotine – Li algorithm works in Gliders in the way that we were excepting and are generally acceptable in the performance of error correction and the convergence of the system, consider that the experiment were develop in a control environmental, as a pool.

In both cases the simulation results and also in real time experiments the parameters that were adapted converge to a constant value, the only difference that in real time experiments were present some oscillation of the value than in simulations results the value were perfectly constant. It is desirable to inquire into various adaptive control techniques, specifically one that ensures that the estimated parameters converge to the real values. Although the advantages by implementing an adaptive control law, is to provide a control that allows us not to know each detail or the full dynamic model. It is well known that the hydrodynamic parameters and the added mass parameters are difficult to know in a exactly way even if we calculate it numerical. All these terms in the modelling, affect directly and working with an adaptive controls generates the adapt system to follow the real system. The prototype had convergence in less time than using other control laws. And thus reduces the path error.

And finally as a future work is to perform a control with more than 3 parameter estimates to generate a more complete adaptive control, although the constraint to implement these is the sensors. To perform the adaptive control is necessary to have a sensor to read the state X or the translational move in X direction, and we could adapt a more complete system in the 2 degrees of freedom.

ACKNOWLEDGMENT

The authors would like to thank Conacyt for the supporting master's scholarship and CINVESTAV that support the prototype develop and technical support and CIDESI for all the technical support during the project.

REFERENCES

[1] N.E. Leonard y J.G. Graver. Model-based feedback control of autonomous underwater gliders. IEEE Journal of Oceanic Engineering, Special Issue on Autonomous Ocean Sampling Networks, Oct 2001.

[2] J.G. Graver y N.E. Leonard. Underwater glider dynamics and control. In Proc. 12th Int. Symposium on Unmanned Untethered Submersible Tech. Durham, NH, 2001.

[3] T.Fossen. Guidance and Control of Ocean Vehicles. John Wiley and Sons, New York, 1995.

[4] T.Fossen. Marine Control Systems., Guidance, Navigation and Control of Ships, Rigs and Underwater Vehicles. New York, 1995.

[5] Elba Dolores Antonio Yañez,. "Pilotaje de un mini submarino con visiona artificial", Tesis de maestría, CINVESTAV. 2012.

[6] Eduardo Campos Mercado, "Auto-localización de un mini-submarino utilizando la visión por computadora", Tesis de maestría, CINVESTAV. 2010.

[7] Jesús Arturo Monroy Anieva, "Auto-localización de un mini-submarino utilizando un sonar", Tesis de maestría, CINVESAV. 2011.

[8] W.J. Gould. A brief history of boat developments. Southampton Oceanography Center. Disponible en http://www.noc.soton.ac.uk/JRD/HYDRO/argo/history.php

[9] Joshua Slocum Society International Inc. (Webpage). Captain Joshua Slocum, The First Man to Sail Around the World Alone.

[10] J. Sherman, R.E. Davis, W.B. Owens, y J. Valdes. The autonomous underewater glider 'Spray'. IEEE Journal of Oceanic Engineering, Special Issue on Autonomous Ocean Sampling Networks, 26(4), Oct 2001.

[11] B.Etkin. Dynamics of Flight. John Wiley and Sons. New York and London, 1959.

[12] Slotine - Li. Stable Adaptive Systems. Ed. Prentice Hall. United States of America, New Jersey, 1989.

[13] Mark W. Spong & M. Vidyasagar. Robot Dynamics and Control. Fisrt Edition. John Wiley and Sons. New York, Chischester, Brisbane, Toronto, Singapore, 1995.

[14] Asher Bender, Daniel Matthew Steinberg, Ariell Lee Friedman, Stefan B. Williams ,Analysis of an Autonomous Underwater Glider, Australian Centre for Field Robotics , University of Sydney, Sydney, NSW 2006.

[15] Pradeep Bhatta. Nonlinear Stability and Control of Gliding Vehicles. A Dissertation Presented to the Faculty of Princeton University in Candidacy for the Degree of Doctor of Philosophy. 2006.

[16] Hassan K. Khalil. Non Linear Systems. Third Edition. Prentice Hall, New Jersey, 2005.

[17] Ali Hussain, N.A., Arshad, M.R., Mohd-Mokhtar, R., 2nd November 2009. Develop- ment of an underwater glider platform. In: Proceedings of the Electrical and Electronic Postgraduate Colloquium (EEPC2009), Universiti Sains Malaysia, Penang, Malaysia.

[18] Ali Hussain, N.A., Ting, M.C., Arshad, M.R., Mohd-Mokhtar, R., Abdullah, M.Z., 2010. Design of an underwater glider platform for shallow-water applications. Int. J. Intell. Def. Support Syst. 3 (3), 186–206.